

Exchange Study of Atomic Krypton and Tetrahedral Semiconductors

D. J. STUKEL, R. N. EUWEMA, AND T. C. COLLINS

Aerospace Research Laboratories, Wright-Patterson Air Force Base, Ohio 45433

AND

VEDENE H. SMITH, JR.

Queen's University, Kingston, Ontario, Canada

(Received 18 June 1969)

Self-consistent orthogonalized-plane-wave (SCOPW) eigenvalues and binding energies (in the Liberman approximation) using Slater's, Kohn and Sham's, and Liberman's exchange approximations are compared with each other and with experiment for ZnS, ZnSe, GaAs, Ge, Si, and CdS. Over-all comparisons are made with relativistic Hartree-Fock (RHF) results on krypton. Calculations adding Carr and Maradudin's static correlation potential to both RHF and SCOPW programs are reported. It is found that while Liberman's exchange simulates RHF most closely in atomic calculations, the eigenvalues resulting from Slater's exchange agree most closely with experiment in our SCOPW calculations.

I. INTRODUCTION

ALTHOUGH many alleged first-principle energy-band calculations have been published, none of those published to date are fundamentally so in character. Until the problems of exchange and correlation are solved, all energy-band calculations will have arbitrary assumptions involved in the way that exchange and correlation are treated. The purpose of this paper is to examine, on the atomic and on the crystalline level, the best known exchange approximations. This examination will show the merit (or lack of it) of the different approximations. The emphasis is on a successful treatment of exchange in the crystalline case, since one can readily perform the Hartree-Fock (HF) calculation in the atomic case. The exchange approximations most applicable to crystalline calculations are due to Slater,¹ to Kohn and Sham² (generalized as the X_α approximation), and to Liberman.³

A successful exchange approximation must satisfy two criteria. First, it must closely simulate the HF results (energies and wave functions) in free atoms for all electron energy levels from the most tightly bound to the most loosely bound electrons. Not only is this a powerful check on the basic physical content of the approximation, but it is necessary in crystalline calculations to use the same Hamiltonian for core and valence states and both should be correct in a meaningful calculation. The second criterion for a successful exchange approximation is that it must give a very good simulation of HF results for the valence and conduction bands of crystals. Consequently, the approximation must be especially good in regions of low electron density where the valence and conduction electrons are found. This second criterion is vital because atomic HF calculations can be easily performed. The whole need for an exchange approximation arises

in the crystalline case where the HF calculations have not yet been performed.

This lack of a crystalline HF calculation would seem to make it difficult to judge the success of exchange approximations in the crystalline case. Consequently, one must know the size of the correlation contribution in both atomic and crystalline calculations. It will be shown that when core relaxation is taken into account, the relativistic Hartree-Fock (RHF) results for atomic krypton match experiment very closely.⁴ An estimate of the correlation correction is made using the method of Lundqvist and Ufford⁵ in which an energy-independent correlation potential of a degenerate electron gas is added to the atomic and crystalline Hamiltonians.

The atomic calculations presented in this paper were done using modified versions of the RHF computer program developed by Mayers and O'Brien⁶ based on the formalism of Grant^{7,8} and the relativistic local exchange computer program developed by Liberman, Waber, and Cromer.⁹ The self-consistent orthogonalized plane wave (SCOPW) programs were developed at Aerospace Research Laboratories (ARL).

The theoretical background of the exchange approximations is discussed briefly in Sec. II. A discussion of the calculation of binding energies (as distinguished from eigenvalues) in the Liberman and Slater approximations is also given in Sec. II. Our SCOPW programs are described in Sec. III, with particular emphasis placed upon the way the Liberman exchange approximation is handled both in the calculation of Liberman eigenvalues and of binding energies in the Liberman approximation. The size of the correlation contribution

⁴ A. Rosén and I. Lindgren, *Phys. Rev.* **176**, 114 (1968).

⁵ S. Lundqvist and C. W. Ufford, *Phys. Rev.* **139**, 1 (1965).

⁶ D. F. Mayers and F. O'Brien, Final Report, The Third Phase of Research on Atomic Structure Project USAF, No. AF33(615)-5203, 1967 (unpublished).

⁷ I. P. Grant, *Proc. Roy. Soc. (London)* **A262**, 555 (1961).

⁸ See also, Y. K. Kim, *Phys. Rev.* **154**, 17 (1967); F. C. Smith and W. R. Johnson, *ibid.* **160**, 136 (1967).

⁹ D. Liberman, J. T. Waber, and D. T. Cromer, *Phys. Rev.* **137**, A27 (1955).

¹ J. C. Slater, *Phys. Rev.* **81**, 385 (1951).

² W. Kohn and L. J. Sham, *Phys. Rev.* **140**, A1133 (1965).

³ D. A. Liberman, *Phys. Rev.* **171**, 1 (1968); L. J. Sham and W. Kohn, *ibid.* **145**, 56 (1966).

in both atomic and crystalline calculations is discussed in Sec. IV. The calculated results are given in Sec. V. The relativistic comparisons of total energy, eigenvalues, and binding energies are presented in the atomic case using krypton as the example. The SCOPW eigenvalues and binding energies (in the Liberman and X_α approximations) are presented for the various exchange approximations with ZnS as the principal example, although some results are also presented for Si, AlP, Ge, GaAs, CdS, and ZnSe. The x-ray form factors, which have been calculated for ZnSe using the different exchange approximations, are compared with experimental results.

II. THEORETICAL BACKGROUND

In the energy-band theory of solids and in atomic and molecular theory, the correct many-body quantum-mechanical equations of motion have not been solved

TABLE I. Expressions are presented for the total energies, Hamiltonians, exchange terms, eigenvalues, and binding energies in the various approximations. Atomic units are used throughout.

| HF: Hartree Fock L: Liberman | S: Slater KS: Kohn-Sham-Gaspar α : Parametrized constant exchange |
|--|--|
| Total energy | |
| $E_T^A = \sum_\mu \langle \mu -\nabla^2 - \frac{2z}{r} \mu \rangle + \frac{1}{2} \sum_{i,j} \langle ij -\frac{2}{r_{12}} ij \rangle + E_X^A$ | |
| $E_X^{\text{HF}} = -\frac{1}{2} \sum_{i,j} \langle ij -\frac{2}{r_{12}} ji \rangle$ | |
| $E_X^L = \frac{1}{2} \sum_i \langle i V_{XL,i} i \rangle$ | |
| $E_X^S = \frac{1}{2} \sum_i \langle i V_{XS} i \rangle$ | |
| $E_X^{\frac{1}{2}\alpha} = \frac{1}{2} \sum_i \langle i \frac{3}{2} V_{X\alpha} i \rangle$ | |
| Hamiltonian | |
| $\mathcal{H}^A = -\nabla^2 - \frac{2z}{r} + \sum_j \int d\tau_2 \Phi_j^*(x_2) \Phi_j(x_2) \frac{2}{r_{12}} + V_{XA}$ | |
| $V_{X\text{HF},i}(\mathbf{r}) = -\sum_j \Phi_j(x_1) \int \Phi_j^*(x_2) \Phi_i(x_2) \frac{2}{r_{12}} d\tau_2 / \Phi_i(x_1)$ | |
| $V_{XL,i}(\mathbf{r}) = -8F(k/k_F) \frac{k_F}{2\pi}; \quad F(\eta) = \frac{1}{2} + \frac{1-\eta^2}{4\eta} \ln \left \frac{1+\eta}{1-\eta} \right $ | |
| $k_F = \{3\pi^2 \rho(\mathbf{r})\}^{1/3} \text{ or } [E_F - V_F(\mathbf{r})]^{1/2}$ $k_i = [E_i - V(\mathbf{r})]^{1/2}$ | |
| $V_{XS}(\mathbf{r}) = -6k_F/2\pi$ | |
| $V_{X\text{KS}}(\mathbf{r}) = -4k_F/2\pi; \quad V_{X\alpha}(\mathbf{r}) = -6\alpha k_F/2\pi$ | |
| Eigenvalues and binding energies | |
| $\mathcal{H}^A i_A\rangle = \epsilon_i^A i_A\rangle$ | |
| $B_{i'A}^C = \langle i_A \mathcal{H}^C i_A \rangle$ | |

except for the simplest systems. Various approximations have been made to reduce the problem to a manageable size. The more complicated the system, the more approximations one uses. The purpose of this section is to outline some of the approximations that are made in electronic systems.

The Hamiltonian for the electronic system is (in atomic units)

$$\mathcal{H} = - \sum_{i=1}^N \nabla_i^2 - \sum_{\alpha,i} \frac{2}{|\mathbf{r}_i - \mathbf{R}_\alpha|} + \sum_{i<j} \frac{2}{r_{ij}}. \quad (2.1)$$

The first term on the right side is the kinetic energy, the second term represents the interaction of the nuclei (or nucleus in the atomic system) with the electrons, and the last term is the electron-electron interaction. The correlated positions of the electrons are neglected when the system wave function is written as an anti-symmetric product of one-electron wave functions (Slater determinant). The resulting HF expression for the total energy becomes (neglecting nucleus-nucleus interactions)

$$E_T^{\text{HF}} = \langle \Psi | \mathcal{H} | \Psi \rangle = \sum_{i=1}^N \langle i | \mathcal{H}_1 | i \rangle + \frac{1}{2} \sum_{i,j=1}^N \left\{ \langle ij | \frac{2}{r_{12}} | ij \rangle - \langle ij | \frac{2}{r_{12}} | ji \rangle \right\}, \quad (2.2)$$

where H_1 includes the kinetic energy of the electron and its potential in the field of all nuclei. The one-electron wave functions Φ_i are determined by requiring that the total energy be a minimum and that the one-electron wave functions be orthogonal to each other, i.e., the HF method. The HF equations obtained for the one-electron wave functions are

$$\begin{aligned} \mathcal{H}_1 \Phi_i(x_1) + \left\{ \sum_{j=1}^N \int d\tau_2 \Phi_j^*(x_2) \Phi_j(x_2) \frac{2}{r_{12}} \right\} \Phi_i(x_1) \\ - \left\{ \sum_{j=1}^N \int d\tau_2 \Phi_j^*(x_2) \Phi_i(x_2) \frac{2}{r_{12}} \right\} \Phi_j(x_1) \\ = \epsilon_i^{\text{HF}} \Phi_i(x_1). \end{aligned} \quad (2.3)$$

One not only obtains the Φ_i 's from the above equation, but also the eigenvalues ϵ_i^{HF} . The ϵ_i^{HF} is equal to the negative of the energy that would be required to remove the i th electron from the system provided that the system did not relax after the electron is removed (Koopmans's theorem).¹⁰ In other words, the eigenvalues ϵ_i^{HF} of the HF equations are equivalent to the binding energies $B_{i,\text{HF}}^{\text{HF}}$, where the binding energies are defined to be

$$\begin{aligned} +B_{i,\text{HF}}^{\text{HF}} &= -E_T^{\text{HF,ion}} + E_T^{\text{HF,ground state}} \\ &= \langle i | \mathcal{H}_1 | i \rangle + \sum_{j=1}^N \left\{ \langle ij | \frac{2}{r_{12}} | ij \rangle - \langle ij | \frac{2}{r_{12}} | ji \rangle \right\}. \end{aligned} \quad (2.4)$$

¹⁰ T. Koopmans, *Physica* **1**, 104 (1939).

The above equations can be solved for free atoms. Correlation can then be accounted for by configuration interaction involving sums of Slater determinants. But for molecular and solid-state calculations, the complexity of the nonlocal HF exchange term necessitates additional approximations. These approximations, which are necessary today, will undoubtedly cease to be necessary when faster and larger computers become available.

The best known approximations to the HF exchange term are due to Slater,¹ to Kohn and Sham² and Gaspar,¹¹ and to Liberman.³ Table I gives expressions for the total energies, Hamiltonians, eigenvalues, and binding energies for all the widely used exchange approximations. This table also gives the nomenclature used in this paper and the equations relevant to the following discussion.

The first simplified one-electron operator which replaces the exchange operator in the HF equation was suggested by Slater.^{1,12} If one multiplies and divides the exchange term in Eq. (2.3) by $\Phi_i^*(x_1)\Phi_i(x_1)$ one has¹³

$$\left\{ - \sum_{j=1}^N \left[\int d\tau_2 \Phi_j^*(x_2) \Phi_i^*(x_1) \Phi_j(x_1) \Phi_i(x_2) \frac{2}{r_{12}} \right] \Phi_i^*(x_1) \Phi_i(x_1) \right\} \Phi_i(x_1) = V_x \Phi_i(x_1). \quad (2.5)$$

In this expression, Slater then made the free-electron gas approximation that the Φ_i are plane waves and obtained

$$V_x(\mathbf{r})|_{\text{FEG}} = -8 \left\{ \frac{3}{8\pi} \rho(\mathbf{r}) \right\}^{1/3} F(k/k_F), \quad (2.6)$$

where $F(\eta)$ is given in Table I and graphed in Fig. 1. $\rho(\mathbf{r})$ is the electron density of the system. Here it has

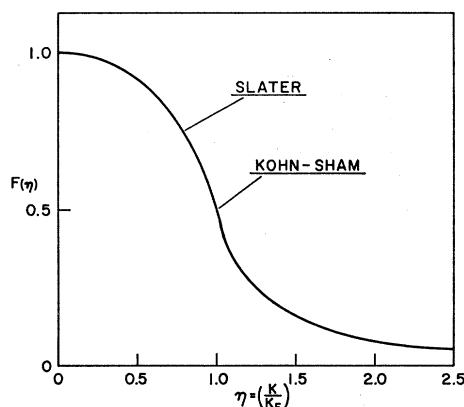


FIG. 1. Function $F(\eta)$ versus η .

¹¹ R. Gaspar, *Acta Phys. Acad. Sci. Hung.* **3**, 263 (1954).

¹² J. C. Slater, in *Quantum Theory of Atomic Structure* (McGraw-Hill Book Co., New York, 1960), Vol. II, Chap. 17, Appendix 22.

¹³ See also the derivation of P. O. Lowdin, *Phys. Rev.* **97**, 1590 (1955).

been assumed that all states are filled for $|\mathbf{k}| < |\mathbf{k}_F|$, the Fermi momentum, and all states are empty for $|\mathbf{k}| > |\mathbf{k}_F|$. The wave vector k and the Fermi wave vector k_F were taken to be

$$k(\mathbf{r}) = \{E - V(\mathbf{r})\}^{1/2}, \quad (2.7)$$

where $V(\mathbf{r})$, the total electronic potential, includes both Coulomb (nuclear and electron) and exchange contributions, and

$$k_F(\mathbf{r}) = \{3\pi^2 \rho(\mathbf{r})\}^{1/3}. \quad (2.8)$$

This definition of k_F is derivable from phase-space considerations. Slater then averaged $F(\eta)$ over the occupied states and obtained the value $\frac{3}{4}$ shown in Fig. 1. Hence,

$$V_{XS}(\mathbf{r}) = -6 \left\{ \frac{3}{8\pi} \rho(\mathbf{r}) \right\}^{1/3}. \quad (2.9)$$

Liberman³ investigated $V_x(\mathbf{r})|_{\text{FEG}}$ with k and k_F given by Eqs. (2.7) and (2.8). Hence,

$$V_{XL,i}(\mathbf{r}) = -8 \left\{ \frac{3}{8\pi} \rho(\mathbf{r}) \right\}^{1/3} F(\eta). \quad (2.10)$$

Slater, Wilson, and Wood¹⁴ modified Liberman's approximation by using

$$k_F(\mathbf{r}) = \left\{ E_F - V_{\text{Coulomb}}(\mathbf{r}) + 4 \left[\frac{3}{8\pi} \rho(\mathbf{r}) \right]^{1/3} \right\}^{1/2} \quad (2.11)$$

instead of Eq. (2.8) so that $\eta=1$ is at the top of the Fermi distribution. We have found it advantageous to calculate k_F both ways and always use the larger value. This approach gives results slightly closer to the HF results for krypton. The value of the Fermi energy E_F that was used in the crystalline calculation was the middle of the fundamental gap, defined by the top of the valence band and the bottom of the conduction band. In the atomic case, E_F was chosen analogously to be zero.¹⁴

One obtains different results when making either of the above exchange approximations, depending upon when the approximation is made. The Liberman or Slater approximation can be made before or after the total energy is varied to obtain the Hamiltonian and differenced to obtain binding energies. The free-electron gas approximation and the variation (or differencing in the case of binding energies) do not commute. This fact is shown in Fig. 2 which gives the relations among the various exchange approximations.

Let us now consider the various paths shown in Fig. 2. If one makes no approximations, the variation of E_T^{HF} with respect to $\Phi_j^*(x_2)$ results in the usual HF Hamiltonian and binding energies. When the Slater approximation is made after the variation [in Eq. (2.3)]

¹⁴ J. C. Slater, T. M. Wilson, and J. H. Wood, *Phys. Rev.* **179**, 28 (1969).

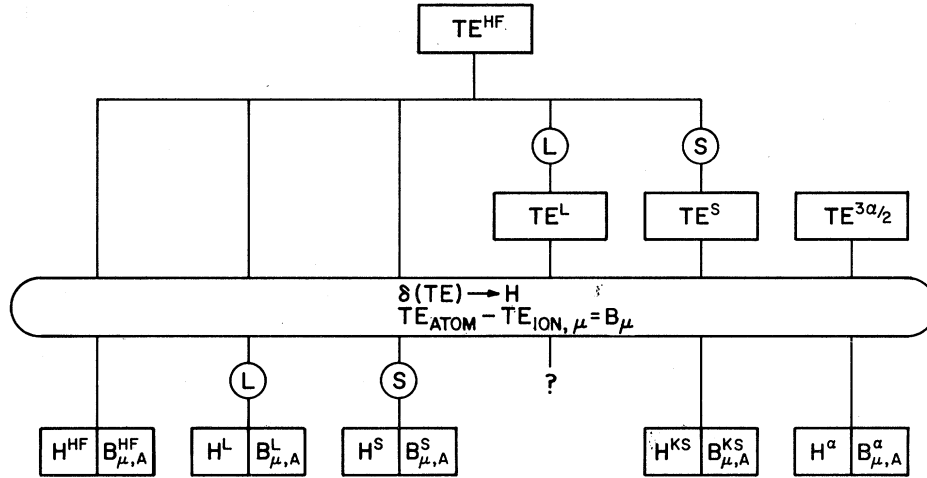


FIG. 2. Outline of the different possible paths in calculating total energies TE, orbitals (H is the Hamiltonian used), and binding energies B. The loop represents either a variation or difference operation. The circle indicates that a free-electron gas approximation was made at that point in the derivation.

one obtains the Hartree-Fock-Slater equations which have eigenvalues ϵ_i^S . If one makes this same approximation after differencing [in Eq. (2.4)], the binding energy $B_{i,S}^S$ is identical to ϵ_i^S . However, if one uses the orbitals obtained from the Hartree-Fock-Slater equations and does not make this approximation in Eq. (2.4), the binding energy $B_{i,S}^{HF}$ will not be identical to the Slater eigenvalues ϵ_i^S .

Whenever a difference occurs between the eigenvalues and binding energies (regardless of the approximations made in calculating them), it is known as a "Koopmans's correction." Obviously, there can be a large number of different Koopmans's corrections, so one must specify both the way the orbitals were obtained and the approximations used in the calculation of the binding energy. Thus the definition used in this paper for Koopmans's corrections K is

$$K_{i,A}^C = B_{i,A}^C - \epsilon_i^A. \quad (2.12)$$

A denotes the approximation used in obtaining the wave functions and C denotes the approximation made in the binding energy calculation. Hence, if one has made Slater's approximation after the variation was performed and after the differencing in Eq. (2.4) for the binding energy, one has no Koopmans's correction, i.e., $K_{i,S}^S = 0$.

From Fig. 2, it is clear that using the same approximation at a different place in the derivation leads to a different path. If one makes Slater's approximation in the exchange term in Eq. (2.2) and then varies the total energy, one obtains the Kohn-Sham-Gaspar exchange approximation^{2,11,15}

$$V_{XKS} = \frac{2}{3} V_{XS}. \quad (2.13)$$

If one makes the Slater approximation before the differencing to obtain the binding energies, the binding energies $B_{i,Ks}^{KS}$ and the eigenvalues ϵ_i^{KS} are the same within a factor $\propto N^{-2/3}$, where N is the total number of

electrons.¹⁶ Therefore, $K_{i,Ks}^{KS} \propto N^{-2/3}$. However, $K_{i,Ks}^S$ is not identically zero, nor is $K_{i,Ks}^{HF}$.

The above procedure has been parameterized^{14,17} by the introduction of a multiplicative factor $\frac{3}{2}\alpha$. If one substitutes $\frac{3}{2}\alpha V_{XS}$ into the total energy equation and then does the variation, one finds the exchange potential¹⁸

$$V_{x\alpha} = \alpha V_{XS}.$$

The parameter α is then adjusted so that the total energy calculated in the HF approximation with these orbitals is minimized. The value of α which give the minimum is denoted α_m .

The above discussion was based on the nonrelativistic Hamiltonian given in Eq. (2.1). In the RHF and local exchange methods for an atom, the operator H_1 is replaced by its Dirac counterpart,

$$\mathcal{H}_1^D = \alpha_1 \cdot \mathbf{p}_1 + \beta_1 C^2 - 2Z/r_1, \quad (2.14)$$

where \mathbf{p}_1 is the momentum of electron 1, and α and β are the Dirac matrices. The one-electron wave functions $\Phi_i(x_i)$ are now of the usual four-component form. The two-particle interaction is the same as in Eq. (2.1). The so-called Breit-Brown¹⁹⁻²¹ magnetic and retardation interactions can be optionally included or excluded. Their effect is negligible for our considerations. These corrections were not included in the results reported here.

III. SCOPW CALCULATION MODEL

The crystalline energy-band calculations were made using modified versions of our basic SCOPW energy-

¹⁶ J. C. Slater, J. B. Mann, T. M. Wilson, and J. H. Wood Phys. Rev. **184**, 672 (1969).

¹⁷ D. J. McNaughton and V. H. Smith, Jr., Int. J. Quantum Chem. (to be published).

¹⁸ W. E. Rudge, Phys. Rev. **181**, 1033 (1969); M. Ross, *ibid.* **179**, 612 (1969).

¹⁹ G. Breit, Phys. Rev. **34**, 553 (1929).

²⁰ G. E. Brown, Phil. Mag. **43**, 467 (1952).

²¹ H. A. Bethe and E. E. Salpeter, *Quantum Mechanics of One- and Two-Electron Atoms* (Academic Press Inc., New York, 1957).

¹⁵ P. Hohenberg and W. Kohn, Phys. Rev. **136**, B864 (1964).

band programs.^{22,23} Following the usual OPW procedure, the electronic states of Zn and S (for example) are divided into tightly bound core states and loosely bound valence states. The core states are calculated using a spherically averaged crystalline potential. There must be no appreciable core overlap between nearest-neighbor atoms. The valence states are expanded in a modified Fourier series,

$$\Psi_{\mathbf{k}_0}(\mathbf{r}) = \frac{1}{\sqrt{\Omega_0}} \sum_{\mu} C_{\mu\nu} \left\{ e^{i\mathbf{k}_\mu \cdot \mathbf{r}} - \sum_a e^{i\mathbf{k}_\mu \cdot \mathbf{R}_a} \right. \\ \left. \times \sum_{n,l} \Phi_{n,l,\mathbf{k}_\mu}(\mathbf{r}-\mathbf{R}_a) A_{n,l,\mathbf{k}_\mu} \right\}, \quad (3.1)$$

$$\mathbf{k}_\mu = \mathbf{k}_0 + \mathbf{K}_\mu,$$

where Ω_0 is the unit-cell volume, \mathbf{k}_0 is a vector in the first Brillouin zone, the \mathbf{K}_μ sum is over all reciprocal-lattice vectors, and the sum over \mathbf{R}_a is over all atoms in the crystal. The sum over nl is over atomic core states,

$$\Phi_{n,l,\mathbf{k}}(\mathbf{r}-\mathbf{R}_a) = \frac{P_{nl}(|\mathbf{r}-\mathbf{R}_a|)}{|\mathbf{r}-\mathbf{R}_a|} Y_{0,k}^l(\theta), \quad (3.2)$$

where $Y_{0,k}^l$ is a spherical harmonic with z axis taken along k , and n and l label the principal and orbital angular quantum numbers of the atomiclike states. The constants $A_{n,l,\mathbf{k}}$ are chosen so that the quantity in brackets, an OPW, is orthogonal to all core-state wave functions. (See Woodruff²² for a more complete discussion of the basic OPW formalism.)

The energy-band calculations reported here have been carried out in a nonrelativistic formalism. The neglect of the relativistic (mass-velocity and Darwin connections) and spin-orbit coupling effects can lead to errors in the calculated band structure, particularly in crystals composed of heavier atoms. This is not the case for ZnS which is used as an example in this paper.

The experimental value of the spin-orbit splitting of the Γ_{15v} level ($\Gamma_8-\Gamma_7$) is 0.065.²⁴ Rough estimates of the relativistic (mass-velocity and Darwin) corrections can be obtained by first-order perturbation theory. Herman²⁵ has done this using his non-self-consistent OPW wave functions. These estimates are given in the last column of Table II. The largest shift is 0.3 eV. It is believed that these calculated shifts are too large and would be smaller if the calculation were carried out self-consistently. In any case, it is clear that even if one accepts these estimates as accurate, for ZnS the relativistic effects are quite small.

TABLE II. SCOPW energy eigenvalues obtained using the L, S, and KS exchange approximations are given in the first three columns. In columns 4 and 5 are given the S and KS binding energies calculated in the Liberman approximation. In column 6, the KS binding energies calculated in the Slater approximation are given. Column 7 gives the change in the L eigenvalues due to the addition of correlation. The last column gives Herman's estimates of the relativistic mass-velocity and Darwin corrections calculated in a non-self-consistent OPW model.^a For ΔE_{Rel} , the zero of energy has been placed at the top of the valence band (Γ_{15v}). All entries are in eV.

| | E_L | E_S | E_{KS} | B_{SL} | B_{KS^L} | B_{KS^S} | ΔE_{corr} | ΔE_{Rel} |
|----------------|-------|-------|----------|----------|------------|------------|--------------------------|-------------------------|
| Γ_{1v} | | -7.00 | -1.76 | -7.12 | -7.31 | -8.26 | | |
| Γ_{15v} | 0.88 | 4.75 | 10.36 | 8.97 | 8.65 | 2.58 | -1.72 | 0.0 |
| Γ_{1c} | 6.48 | 8.46 | 13.08 | 13.98 | 13.24 | 7.40 | -1.51 | -0.3 |
| Γ_{15c} | | 12.63 | 17.08 | 19.01 | 18.89 | 11.91 | | 0.0 |
| X_{1v} | | -5.48 | 0.04 | -4.28 | -5.16 | -7.93 | | |
| X_{3v} | | 0.77 | 5.80 | 2.61 | 2.52 | -0.70 | | |
| X_{5v} | -1.93 | 3.12 | 8.26 | 6.07 | 6.06 | 1.89 | -1.69 | 0.0 |
| X_{1c} | 8.09 | 9.66 | 13.78 | 14.57 | 14.02 | 8.68 | -1.73 | 0.0 |
| X_{1c} | 9.26 | 10.59 | 15.38 | 16.59 | 16.18 | 9.44 | -1.46 | -0.2 |
| L_{1v} | | -5.87 | -0.43 | -4.96 | -5.77 | -8.25 | | |
| L_{1v} | | 0.49 | 5.27 | 1.93 | 1.99 | -0.45 | | |
| L_{3v} | -0.15 | 4.13 | 9.56 | 7.86 | 7.70 | 2.37 | -1.73 | 0.0 |
| L_{1c} | 8.10 | 9.62 | 14.21 | 15.30 | 14.83 | 8.61 | -1.49 | -0.3 |
| L_{3c} | | 13.27 | 17.72 | 19.81 | 19.50 | 12.39 | | 0.0 |

^a See Ref. 25.

These two requirements of no core overlap and convergence of the valence Fourier series with a reasonable number (about 250) of OPW's determines the division into core and valence states. In ZnS, the Zn4s states and the S3s and 3p states are considered valence states. As we showed in detail in two previous papers,^{23,25} core overlap is then negligible and the Fourier series has adequately converged by 229 OPW's.

The calculation is self-consistent in the sense that core and valence state energies and wave functions are calculated alternately with appropriate updating of crystalline potential and orthogonality coefficients, $A_{n,l,\mathbf{k}}$, until the valence energies change less than 0.01 eV from iteration to iteration. In calculating the contribution to the crystalline potential made by the valence electron density, the electron density average over the Brillouin zone is estimated by a weighted average over the four symmetry points, Γ , X , L , and W , of the zinc-blende Brillouin zone. The adequacy of this four-point weighting is discussed at some length in a paper comparing the ARL SCOPW results with x-ray charge densities to be published with Raccach.²⁶ Because the band energies are only calculated at the high symmetry points in the SCOPW method, the high-symmetry-point results are extended throughout the Brillouin zone using a pseudopotential interpolation procedure.²⁷ The pseudopotential results are used to calculate the imaginary part of the dielectric constant ϵ_2 . The comparison of the calculated ϵ_2 peak positions

²² T. O. Woodruff, in *Solid State Physics*, edited by F. Seitz and D. Turnbull (Academic Press Inc., New York, 1957), Vol. V, p. 367.

²³ R. N. Euwema, T. C. Collins, D. G. Shankland, and J. S. DeWitt, *Phys. Rev.* **162**, 710 (1967).

²⁴ J. L. Birman, H. Samelson, and A. Lempicki, G. T. E. Res. Develop. **J. 1**, 2 (1961).

²⁵ D. J. Stukel, R. N. Euwema, T. C. Collins, F. Herman, and R. L. Kortum, *Phys. Rev.* **179**, 740 (1969).

²⁶ P. M. Raccach, R. N. Euwema, D. J. Stukel, and T. C. Collins *Phys. Rev.* (to be published).

²⁷ R. N. Euwema, D. J. Stukel, T. C. Collins, J. S. DeWitt, and D. G. Shankland, *Phys. Rev.* **178**, 1419 (1969).

with the experimental results allows a good judgment of the accuracy of the calculated bands.

The exchange potential for the X_α case is treated in the following way. A valence wave function is written as the sum of plane-wave terms Φ_{pw} , and the sum of terms involving the core wave functions Φ_{v-c} :

$$\Phi_v = \Phi_{pw} + \Phi_{v-c}.$$

The valence electron density ρ_v can be written

$$\rho_v = \sum |\Psi_v|^2 = \sum |\Phi_{pw}|^2 + \sum [(\Phi_{pw}^* \cdot \Phi_{v-c}) + (\Phi_{v-c}^* \cdot \Phi_{pw}) + (\Phi_{v-c}^* \cdot \Phi_{v-c})] \equiv \rho_{pw} + \rho_{v-c}. \quad (3.3)$$

Throughout the self-consistent calculation, the ρ_{v-c} term is spherically symmetrized. When calculating new core states, ρ_{pw} is also spherically symmetrized about each inequivalent site and $\rho^{1/3}$ is calculated. For the valence calculation, $V_x(k)$ is needed. The total electron charge density is written

$$\rho^{1/3} = [\rho^{1/3} - (\rho_{v-c} + \rho_c)^{1/3}]_{\text{Crystal mesh}} + (\rho_{v-c} + \rho_c)^{1/3}_{\text{Atomic mesh}}. \quad (3.4)$$

The first term is calculated over an appropriate crystalline mesh of 650 points in $1/24$ of the Brillouin zone and is Fourier transformed by the three-dimensional generalization of the formulas

$$f_p = \sum_{j=-N}^N g(j) e^{2\pi i j p / (2N+1)}, \quad (3.5)$$

$$g(j) = \frac{1}{2N+1} \sum_{p=-N}^N f_p e^{-2\pi i j p / (2N+1)}.$$

The last term in Eq. (3.4) which is spherically symmetric about each atom site is calculated in the usual way,

$$f(\mathbf{k}) = \sum_a e^{2\pi i \mathbf{k} \cdot \mathbf{R}_a} \int d\mathbf{r} g(r) \frac{\sin kr}{kr} 4\pi r^2, \quad (3.6)$$

where the sum is over atoms in the unit cell.

The calculation involving the L exchange approximation is more involved because a separate exchange potential is needed for each state due to the occurrence of E_μ in the relation $k^2 = [E_\mu - V(r)]$, used in $F(k/k_F)$. In the core calculation, ρ_{pw} is again spherically symmetrized and the calculation proceeds using the appropriate core energy in each case. For the valence state calculation, this procedure would be too cumbersome. Consequently, a weighted average of high-symmetry-point valence-band energies is taken and this value is used for E_μ in the expression for k^2 for all valence states. A study of the effect of varying this E_v from the bottom to the top of the valence band found no appreciable change in the valence charge density.

It was found that the decomposition of ρ in Eq. (3.4) into a smoothly varying crystal mesh part and a spherically symmetrical core part gave misleading

results in the L calculation because of the slightly different $F(\eta)$ in the two cases (because of spherically symmetrizing ρ_{pw} in the core part). Consequently, a much finer crystalline mesh of 1785 points in $1/24$ of the Brillouin zone was used. The total quantity $F(\eta)\rho^{1/3}$ was evaluated at each crystalline mesh point, and then Fourier transformed according to the formulas of Eq. (3.5).

A complication arises because of the nonorthogonality of the L wave functions due to the different Hamiltonian used for the different states. The SCOPW method requires that the same Hamiltonian be used for core and valence calculations, or more explicitly the variational solution of the valence problem requires that the functions Φ_{nl,k^a} in Eq. (3.1) be solutions of the valence Hamiltonian. The problem is solved in the following way. The core density is determined with the usual L prescription (different H for each state). This core density is then used to determine the updated crystalline potential. When the core states are mutually self-consistent, one final core wave function calculation is performed with the previously determined core density, but with all the E_μ taken equal to E_v in the expression $k^2 = E_v - V(r)$ in $F(\eta)$. The resulting Φ_{nl,k^a} are solutions of the valence Hamiltonian and are used in Eq. (3.1) along with the corresponding A_{nl,k^a} and $E_n l^c$.

While the preceding technique is sufficiently accurate to determine the valence electron density, the variation of E_μ with E_v must be taken into account when finding the final valence and conduction-band eigenvalues. This final eigenvalue determination is made by freezing

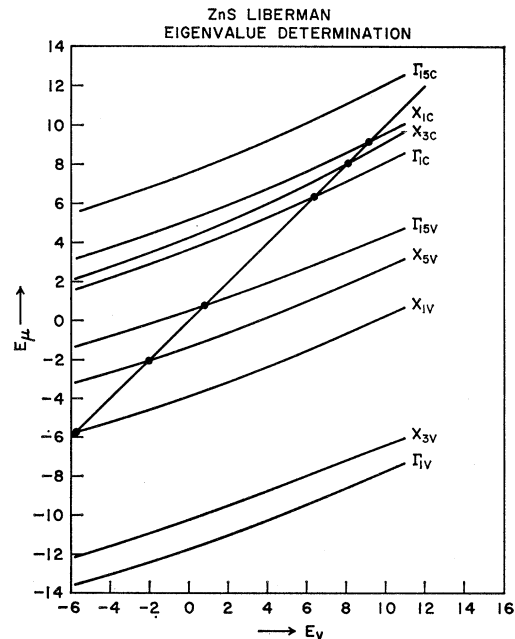


FIG. 3. Eigenvalue E_μ versus value of E_v in $k = (E_v - V)^{1/2}$. The 45° line crossing gives the correct E_μ value.

the self-consistent crystalline charge density, both valence and core. Then the calculation is continued with the determination of new orthogonality functions A_{nl,k^a} through the calculation of the crystal-mesh exchange potential, and through the valence eigenvalue calculation using each of four E_v 's in $F(\eta)$. The resulting eigenvalues, when plotted as a function of E_v , are shown in Fig. 3 for the case of ZnS. The intersection of the curves $E_\mu(E_v)$ with the 45° line $E_\mu = E_v$ then gives the required L eigenvalues, i.e., the solution where $k^2 = E_\mu - V(r)$ is used in determining $F(\eta)$ in the exchange potential.

For the crystalline binding-energy calculation (in the Liberman or Slater approximation), the desired binding energies are related to the X_α eigenvalues by the equations

$$\begin{aligned} B_{i,\alpha}^{\text{L or S}} &= \epsilon_i \alpha + \int \Psi_i^*(r) [V_{XL \text{ or } XS} - V_{x\alpha}] \Psi_i(r) dr \\ &= \epsilon_i \alpha + \int \rho_i(r) [V_{XL \text{ or } XS} - V_{x\alpha}] dr \\ &= \epsilon_i \alpha + \int [\rho_{i,\rho\omega} + \rho_{i,v-c}] [V_{XL \text{ or } XS} - V_{x\alpha}] dr. \end{aligned}$$

The first integral is performed numerically over a crystalline mesh of 1485 points, while the second integral is evaluated for each inequivalent atom. The appropriate E_μ is used for E_v in $k^2 = E_\mu - V(r)$ for each valence state.

IV. HARTREE-FOCK CORRELATION AND EXPERIMENT

In this section, we present evidence that the contribution is very small relative to the deviations between the various exchange approximations for atoms. We also show for krypton that when relaxation of the core states is properly considered, the RHF results match experiment much more closely than any of the exchange approximation results (with the exception of those exchange approximations that match RHF).

The proper way to calculate ionization energies for various electronic energy levels of an atom is to subtract the total energy of the self-consistent atom from that of the self-consistent ion. This is the only correct way to handle the relaxation of the electronic wave functions. It should be noted that both the atom and ion calculations were done in the restricted formalism (assuming spherical symmetry) which is correct for the closed-shell krypton but is less valid for the ion. RHF calculations were carried to self-consistency for atomic krypton and separately for each krypton ion obtained by removing one electron from each atomic state in turn. The resulting ionization energies, obtained by subtracting total energies of atom and ion, are given in column 3 of Table III. The RHF eigenvalues (column 4) for the

TABLE III. Atomic krypton. The experimental ionization energies (of Ref. 28) obtained by electron (Expt.) and by optical spectra (Expt.) are given in columns 1 and 2. The relaxed RHF ionization energies are given in column 3, and the RHF eigenvalues are given in column 4. The L, S, α_M (0.70), and KS eigenvalues are given in columns 5-8. The L, S, α_M , and KS binding energies calculated in the Hartree-Fock approximations are given in columns 9-12. The S, α_M , and KS binding energies calculated in the Liberman and $3\alpha/2$ approximations are given in columns 13-15 and 16-18, respectively. Derivatives of the RHF total energy with respect to the occupation numbers are given in column 19. The change in the RHF eigenvalues due to the addition of correlation is given in column 20. The E_T entries for columns 4, 9-12 give RHF total energies; columns 5, 13-15 give L total energies; and columns 16-18 give $3\alpha/2$ total energies. All entries are in Ry.

| | 1 | 2 | 3 | 4 | 5 | 6 | 7 | 8 | 9 | 10 | 11 | 12 | 13 | 14 | 15 | 16 | 17 | 18 | 19 | 20 |
|-------------------|---------|-------|------------------|------------------|----------|---------|----------------|----------|-----------|-----------|-------------------|-------------|----------|------------------|------------|-------------------|--------------------------|--------------------|---------------------------------|--------------------------|
| | Expt. | Expt. | I_{RHF} | E_{RHF} | E_L | E_S | $E_{\alpha M}$ | E_{KS} | B_{LHF} | B_{SHF} | $B_{\alpha M HF}$ | $E_{KS HF}$ | B_{SL} | $B_{\alpha M L}$ | $B_{KS L}$ | $B_{S 3\alpha/2}$ | $B_{\alpha M 3\alpha/2}$ | $B_{KS 3\alpha/2}$ | $\partial E_T / \partial q_\mu$ | ΔE_{corr} |
| 1s | 1052.99 | | 1055.36 | 1059.39 | 1038.81 | 1049.52 | 1039.49 | 1038.38 | 1060.08 | 1056.31 | 1059.25 | 1059.57 | 1055.04 | 1057.97 | 1058.30 | 1071.28 | 1054.66 | 1052.82 | 1036.69 | 0.18 |
| 2s | 141.20 | | 142.11 | 144.16 | 143.96 | 139.76 | 136.94 | 136.63 | 144.52 | 141.98 | 144.05 | 144.28 | 141.42 | 143.49 | 143.72 | 148.02 | 142.67 | 142.08 | 139.21 | 0.15 |
| 2p ^{3/2} | 126.94 | | 127.51 | 129.75 | 130.13 | 126.98 | 123.90 | 123.57 | 130.16 | 127.45 | 129.65 | 129.90 | 127.39 | 129.60 | 129.85 | 135.87 | 130.07 | 129.44 | 123.95 | 0.15 |
| 2p ^{1/2} | 123.12 | | 123.42 | 125.76 | 126.07 | 122.92 | 119.94 | 119.62 | 126.16 | 123.48 | 125.66 | 125.90 | 123.37 | 125.55 | 125.80 | 131.63 | 125.98 | 125.36 | 117.42 | 0.15 |
| 3s | 21.24 | | 21.77 | 22.45 | 22.23 | 20.39 | 19.32 | 19.20 | 22.58 | 21.37 | 22.42 | 22.54 | 21.01 | 22.06 | 22.18 | 24.01 | 21.81 | 21.58 | 20.74 | 0.13 |
| 3p ^{3/2} | 16.39 | | 16.56 | 17.24 | 17.16 | 15.75 | 14.70 | 14.59 | 17.38 | 16.15 | 17.22 | 17.33 | 15.92 | 16.99 | 17.11 | 19.36 | 17.18 | 16.95 | 15.54 | 0.14 |
| 3p ^{1/2} | 15.73 | | 15.92 | 16.63 | 16.54 | 15.15 | 14.12 | 14.01 | 16.76 | 15.55 | 16.60 | 16.71 | 15.32 | 16.37 | 16.49 | 18.68 | 16.55 | 16.32 | 14.12 | 0.13 |
| 3d ^{5/2} | 6.54 | | 6.83 | 7.56 | 7.57 | 6.94 | 6.03 | 5.94 | 7.70 | 6.47 | 7.53 | 7.65 | 6.32 | 7.39 | 7.51 | 10.32 | 8.33 | 8.12 | 5.09 | 0.13 |
| 3d ^{3/2} | | | 6.73 | 7.45 | 7.46 | 6.84 | 5.94 | 5.84 | 7.60 | 6.37 | 7.43 | 7.55 | 6.22 | 7.29 | 7.41 | 10.19 | 8.22 | 8.01 | 4.50 | 0.13 |
| 4s | 1.76 | | 2.28 | 2.38 | 2.38 | 1.97 | 1.64 | 1.61 | 2.41 | 2.08 | 2.38 | 2.41 | 2.02 | 2.38 | 2.38 | 3.06 | 2.38 | 2.31 | 1.81 | 0.11 |
| 4p ^{3/2} | 0.89 | 1.078 | 1.006 | 1.083 | 1.095 | 0.938 | 0.658 | 0.630 | 1.103 | 0.837 | 1.077 | 1.102 | 0.799 | 1.058 | 1.090 | 1.850 | 1.257 | 1.195 | 0.610 | 0.11 |
| 4p ^{1/2} | 1.029 | 1.029 | 0.943 | 1.029 | 1.033 | 0.884 | 0.610 | 0.582 | 1.048 | 0.791 | 1.021 | 1.045 | 0.747 | 0.997 | 1.028 | 1.772 | 1.191 | 1.131 | 0.327 | 0.11 |
| E_T | | | | 5577.768 | 5699.734 | | | | 5577.667 | 5577.111 | 5577.683 | 5577.676 | 5566.860 | 5567.557 | 5567.564 | 5658.057 | 5576.555 | 5567.564 | | |

atom are also given together with the eigenvalues (column 5–8) and binding energies (column 9–18) obtained from various exchange approximations. The derivatives of the RHF total energy with respect to the occupation number are given in column 19. These quantities are discussed at length in Ref. 16. The experimental ionization energies obtained by electron emission (Expt_A) and by optical spectra (Expt_B) are also given in columns 1 and 2.²⁸

The well-known theorem that the relaxed ionization energy is smaller than the frozen ionization energy is illustrated by comparing the RHF eigenvalues of column 4 (which by Koopmans's theorem give the ionization energies assuming frozen wave functions) with the relaxed ionization energies of column 3 obtained by subtracting total energies. Taking relaxation into account markedly improves the agreement between RHF results and experiment. The deviation is largest for the *s* levels.

Further improvement in the agreement is obtained by considering radiative effects (the Lamb shift). For example, in mercury, the Lamb shift lowers the ionization energy of the 1*s* state by 38 Ry.⁷ A rough estimate for krypton can be obtained from the fact that the Lamb shift goes as $N^4 q^5 mc^2$, where N is the number of electrons and q is the fine structure constant. Scaling the 38 Ry down for krypton then gives roughly 1.6 Ry for the further decrease in the calculated ionization energy due to the Lamb shift. This clearly is of the correct order of magnitude to explain the 2.4-Ry discrepancy between the relaxed RHF calculation and the experimental value. For the 4*p* states, there is an experimental discrepancy between the electron emission results and the optical results. Clearly the optical results are more reliable because of the complicated electron-electron interactions that are so important at low energies for the electron results. Even the 3*d* and 4*s* electron-emission results are suspect when compared to the relaxed RHF results when one realizes the remarkable agreement of the relaxed RHF results with experiment-electron emission at the low end and optical measurements at the upper end.

Thus, the relaxed RHF calculation with allowance for the Lamb shift at the low end agrees exceptionally well with experiment. If one applies the same corrections for relaxation and Lamb shift to the *S* eigenvalues, it is clear that the superficial original agreement becomes much worse. While these corrections move the HF results into agreement with experiment, the same corrections move the *S* results (and even more so the $X_{\alpha m}$ and KS eigenvalues) away from experiment. We observe that *S* eigenvalues do account for atomic-core relaxation.

²⁸ K. Siegbahn *et al.*, Nova Acta Regiae Societates Scientiarum Upsalienses, Series IV, Vol. 20, 1967 (unpublished); C. E. Moore, in *Atomic Energy Levels* (U. S. Government Printing Office, National Bureau of Standards, Washington, D. C., 1952), Circular No. 467, Vol. II.

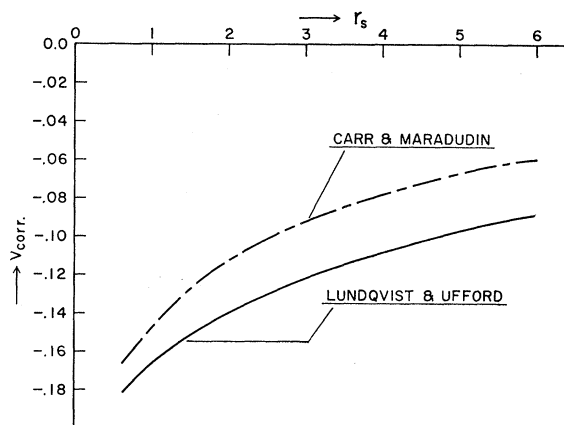


FIG. 4. Static correlation potential versus r_s , the radius of a sphere containing one electron in a free-electron gas. This figure was taken from Lundqvist and Ufford (Ref. 5).

The question then arises as to the magnitude of correlation effects. In the absence of a full-fledged configuration interaction calculation or a Hylleraas calculation, a very rough estimate can be obtained by following the procedure of Lundqvist and Ufford.⁵ They used an energy-independent correlation potential derived for a degenerate electron gas, interpolated between the high- and low-density limits. Figure 4 (taken from Ref. 5) shows two such correlation potentials. We chose the more rapidly varying potential of Carr and Maradudin²⁹ to maximize the effect of correlation and added the potential to the self-consistent RHF programs. (It is clearly better to add this potential to the RHF Hamiltonian where exchange is handled correctly, rather than to the Slater Hamiltonian as Lundqvist and Ufford did where exchange is treated poorly.) The resulting shifts in the RHF eigenvalues, shown in column 20 of Table III, are reasonable if one examines Fig. 4. The deepest electron states are in regions of high electron density and undergo shifts of 0.15 Ry, while the most loosely bound electrons are in regions of low electron density and undergo smaller shifts. While we do not take the actual numbers too seriously, we believe that they indicate the magnitude of the atomic correlation corrections. It is interesting to note that the relaxed RHF 4*p* energies are slightly smaller than the experimental optical results, which is reasonable since correlation should lower the total energy of the 36 electron atom more than the total energy of the 35 electron ion, thus slightly increasing the RHF ionization energy. The actual calculated correlation correction of 0.11 Ry for the 4*p* states is not far from what is actually required (0.09 Ry for the 4*p*^{3/2} and 0.07 Ry for the 4*p*^{1/2}).

We thus conclude that in atomic calculations, RHF energies agree very closely with experiment for all

²⁹ W. J. Carr, Jr., and A. A. Maradudin, *Phys. Rev.* **133**, 371 (1964); G. Pratt, *ibid.* **118**, 462 (1960); L. Hedin, *ibid.* **129**, A796 (1965); L. J. Sham and W. Kohn, *ibid.* **145**, 561 (1966).

states from the most tightly bound to the most loosely bound, and that the correlation corrections are very small, of the order of 0.1 Ry. We further conclude that in the atomic case, the S eigenvalues no longer closely match experiment when core relaxation and the Lamb shift are properly taken into account.

The estimation of the approximate size of correlation in crystals is much more difficult. We added the same energy-independent correlation potential to our SCOPW programs, using the L exchange. The L exchange was chosen because it is the closest approximation to the HF exchange for atomic systems. Also the energy-band eigenvalues obtained using the L exchange show the wide spread effect that one obtains when calculating a HF electron gas. The calculation for ZnS was carried to self-consistency. The resulting shifts (in eV) in the L eigenvalues are shown in Table II. If correlation could be roughly simulated in this fashion, it would only shift band-energy differences by the order of 0.4 eV. However, from the many-body theory, the correlation contribution to the electron self-energy is energy dependent²⁹ and the use of the approximation of the energy-independent correlation potential to calculate the one-electron energy underestimates the band-energy difference. Thus, we can only state that this is a very rough estimate of the energy shifts.

V. RESULTS

A. Total Energy

A very sensitive test of the wave functions obtained from the various exchange approximations is to use them in the calculation of the total energy of an atom. The results of this calculation for krypton are shown in Fig. 5 and summarized in the last row of Table III.

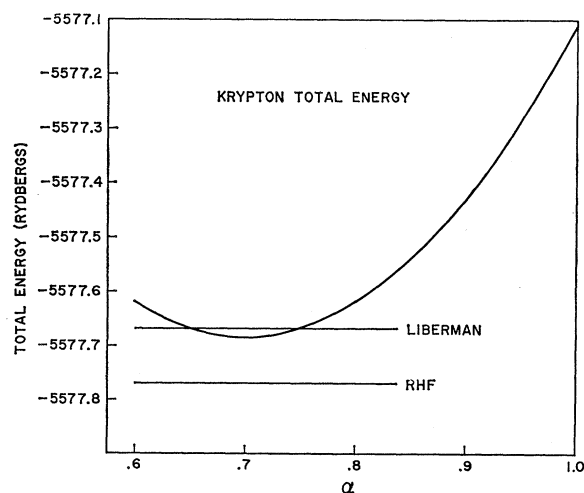


FIG. 5. The total energy calculated in the HF approximation using orbitals obtained from RHF solutions, Liberman solutions and X_α solutions. α varies from the Kohn and Sham value to the Slater value. The energies are in Ry.

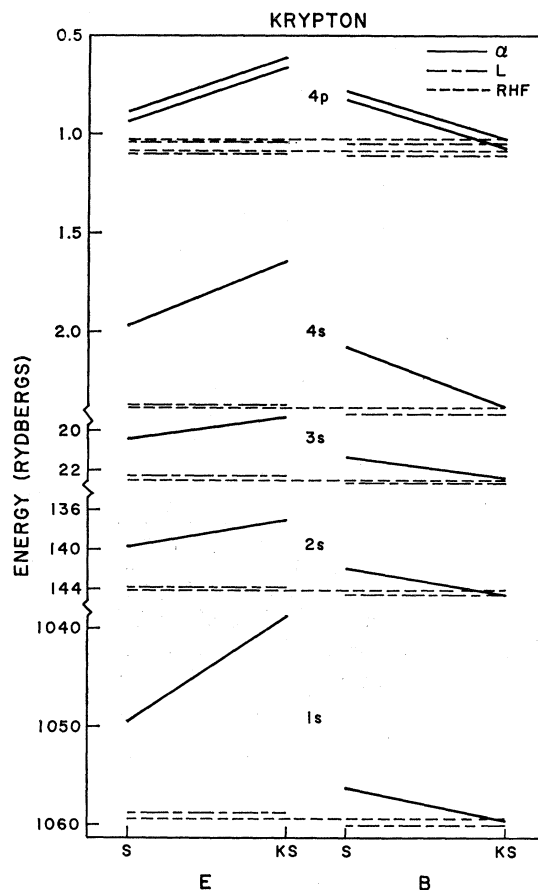


FIG. 6. The variation of the eigenvalues and binding energies of krypton using the RHF, L, and α exchange term. α varies from the Kohn and Sham value to the Slater value. The energies are in Ry.

The exchange coefficient (α_m), which gives the lowest total energy, is 0.70. This coefficient is very close to the free electron value of $\frac{2}{3}$. From Fig. 5 it can be seen that the L, the KS, and the α_m wave functions all give about the same total energy which is still considerably above the RHF value. The difference between this energy and the RHF energy is about one-fifth that of the S to KS difference.

B. Eigenvalues

Krypton eigenvalues for various exchanges are given in columns 4-8 of Table III and representative samples are shown in Fig. 6. The eigenvalues vary almost linearly with the exchange coefficient and increase from S to KS. The KS energy levels are much too compressed to match experiment, the S levels are somewhat too compressed, while L and RHF energy levels are spread out the most and match experiment the closest. The close agreement between the L and RHF eigenvalues is impressive.

It is interesting to note that if the Fermi energy E_F which is used in Eq. (2.11) had been chosen equal to

the $4p$ energy, the L eigenvalue would be almost equal to the KS value for the $4p$ eigenstate because $\eta \cong 1$ for all values of r . Thus, the choice of E_F used in the calculation seems better because the L eigenvalues match the HF eigenvalues well.

Comparable SCOPW results are shown in Figs. 7 and 8(a) and 8(b) and Table II. Figure 7 shows that again the dependence of eigenvalue upon exchange coefficient is linear, with the S eigenvalues again the lowest. We find the same spreading characteristics. The KS bands are closest together, with the S bands next closest. The L bands are the most widely spread out. These statements are generally true, although exceptions can be seen in Figs. 8(a) and 8(b). The dependence of the individual bands upon the exchange coefficient depends upon the character of the bands (symmetry, p -state content, etc.) rather than upon their energy as can be seen from the behavior of the Γ_{15c} and $\Gamma_{2c'}$ states in Ge [Fig. 8(a)] and Si [Fig. 8(b)]. The behavior of Γ , X , and L point bands for the two isoelectronic sequence Si , AlP and Ge , $GaAs$ and $ZnSe$ are shown to give a general idea of the behavior of the various bands with α for different compounds.

In the atomic case, the most widely spread energy levels, those of L and RHF , match experiment most closely. In the case of our SCOPW semiconductor calculations, the S bands have just the correct amount of spread. This point is illustrated in Table IV, where experimental and theoretical band gaps are given. It can be seen that in the case of almost every semiconductor for which we have SCOPW results, the S band gap is within 0.2 eV of experiment, while the L gap is far too large and the KS gap is usually too small. When we go from a non-self-consistent potential to a self-consistent potential, the bands tend to come closer together. The same effect can be obtained for

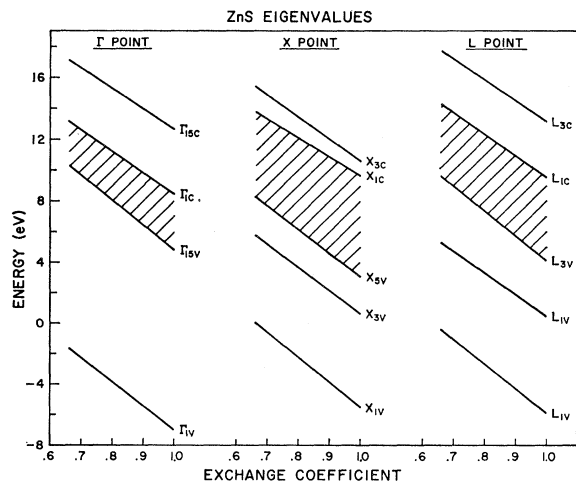


FIG. 7. The variation of the Γ , X , and L high-symmetry-point eigenvalues of ZnS using the X_α exchange term. α varies from the Kohn and Sham value to the Slater value. The energies are in eV.

these crystals by decreasing the exchange coefficient. This tends to explain why in non-self-consistent calculations, KS eigenvalues are closer to experiment than S eigenvalues. Clearly the only physically meaningful comparison is that of self-consistent results with experiment. Few other direct transition energies are known experimentally to compare with the SCOPW results, but we have made comparisons of ϵ_2 curve peak positions which depend upon the bands throughout

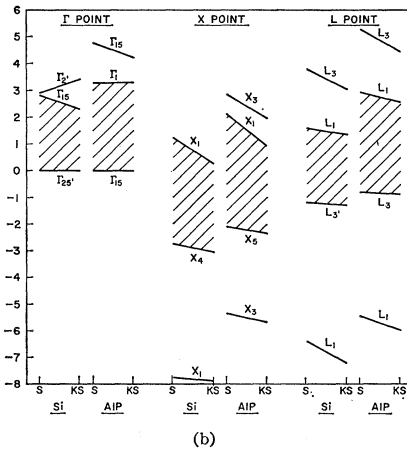
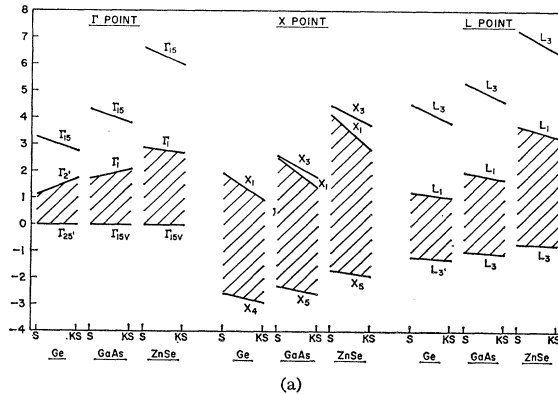


FIG. 8. (a) The variation of the Γ , X , and L high-symmetry-point eigenvalues of Ge , $GaAs$, and $ZnSe$ versus the exchange parameter α . α varies from the Kohn and Sham value to the Slater value. The energies are in eV. (b) The variation of the Γ , X , and L high-symmetry-point eigenvalues of Si and AlP versus the exchange parameter α . α varies from the Kohn and Sham value to the Slater value. The energies are in eV.

the Brillouin zone. There again, as we reported in several papers,^{25,30-32} the S results closely match experiment as to peak positions, while the KS results are compressed at too small energies. The L results again are far too expanded. For some reason not yet com-

³⁰ D. J. Stukel, R. N. Euwema, and T. C. Collins, *Int. J. Quant. Chem.* (to be published).

³¹ T. C. Collins, D. J. Stukel, and R. N. Euwema, *Phys. Rev.* (to be published).

³² D. J. Stukel and R. N. Euwema, *Phys. Rev.* **186**, 754 (1969).

pletely understood in the crystalline case, S results are remarkably good.

C. Binding Energies

Atomic binding energies, shown in columns 9–18 of Table III and Fig. 6, again vary linearly with exchange coefficient. The variation of the upper binding energy levels is comparable to the variation of the eigenvalues, but is in the opposite direction. The KS binding energies very closely match the RHF results, and hence match experiment, while the S binding energies are too high. The binding energies in the L approximation (columns 13–15) agree very closely with the binding energies calculated with the proper RHF Hamiltonian (columns 9–12), partially justifying our use of the L approximation in the crystalline case.

TABLE IV. Direct band gaps (indirect where indicated) are given based on the free atomic and the SCOPW models for different exchange approximations. The experimental value is also given. All entries are in eV.

| Compound | Free atomic | | Self-consistent | | | Expt |
|------------------------------------|-------------|---------------|-----------------|---------------|---------------|-------------------|
| | Slater | Kohn and Sham | Slater | Kohn and Sham | Liber- man | |
| ZnS | 4.30 | 3.68 | 3.71 | 2.72 | 5.60 | 3.84 ^a |
| ZnSe | 3.16 | 2.78 | 2.94 | 2.68 | 4.97 | 2.83 ^b |
| GaAs | 1.32 | 1.49 | 1.61 | 1.97 | 3.63 | 1.54 ^c |
| Si(Δ_1^M - Γ_{25}) | | | 1.10 | 0.10 | 0.94 | 1.12 ^d |
| Ge(L_1 - Γ_{25}) | | | 1.27 | 1.01 | | 0.66 ^e |
| (Γ_2' - Γ_{25}) | | | 1.18 | 1.73 | | 0.80 ^e |
| CdS | | | 2.50 | | | 2.58 ^f |

^a See Ref. 24.

^b M. Aven, D. Marple, and B. Segall, J. Appl. Phys. Suppl. **32**, 226 (1961).

^c M. Cardona, K. L. Shaklee, and F. H. Pollak, Phys. Rev. **154**, 696 (1967).

^d A. Frova and P. Handler, Phys. Rev. Letters **14**, 178 (1965).

^e G. G. MacFarlane, T. P. McLean, J. E. Quarrington, and V. Roberts, Proc. Phys. Soc. (London) **71**, 863 (1958).

^f D. G. Thomas and J. J. Hopfield, Phys. Rev. **116**, 573 (1959).

The dependence of ZnS binding energies on the exchange coefficient, shown in Fig. 9, is not quite linear—some bowing is evident—and the variation is much smaller than the variation of the eigenvalues. All the binding energies, like the L eigenvalues, are much too widely spread out as compared to experiment. For example, the ZnS binding-energy band gap is around 5.6 eV, whereas the experimental value is 3.84 eV.²⁴

The ZnS KS binding energies, calculated in the S approximation, are again too widely spread out, but the high-energy spreading is much less than for the binding energies calculated in the L approximation. The spreading at the high-energy end for both L eigenvalues and binding energies in the L approximation reflects the fact that the $F(\eta)$ curve of Fig. 1 goes rapidly to zero beyond the Fermi energy (where $\eta=1$). The very rapid decrease tends to widely spread out the conduction bands in these crystalline calculations. We conclude that this behavior, which is not tested in

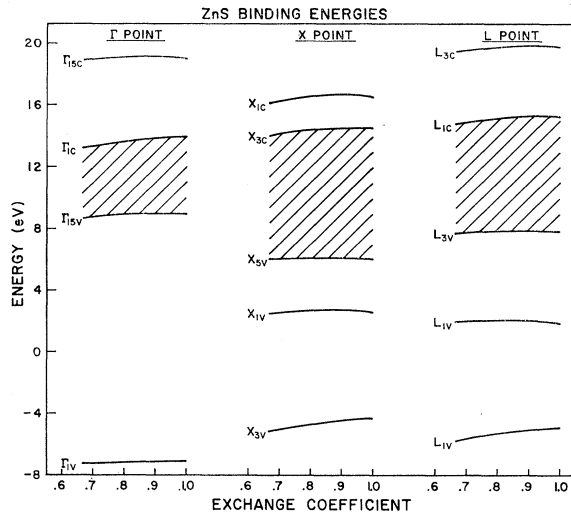


FIG. 9. The variation of the Γ , X, and L high-symmetry-point binding energies of ZnS using X_α exchange term to calculate the orbitals and Liberman's approximation to calculate the binding energies, α varies from the Kohn and Sham value to the Slater value. The energies are in eV.

atomic calculations (where η is always less than 1), is unrealistic.

D. Wave Functions

Another good test of wave functions, in addition to the calculation of total energies is to calculate the Fourier transform of the electron-charge density. The results for free atomic zinc and selenium packed in a crystal lattice (RHF) and SCOPW results for S, KS, and L exchanges are compared with the experimental measurements of Raccach²⁶ in Table V. At high k , ($k^2=4\pi^2/a^2[h^2+k^2+l^2]$), the core-state density is emphasized, while the small k values emphasize the valence contribution. Since the core states are very close to free atomic states, we again have an atomic-

TABLE V. ZnSe form factors. Experimental form factors are taken from Raccach.^a Theoretical form factors are given based on RHF and the SCOPW using the L, S, and KS exchange approximations.

| hkl | Expt | RHF | L | S | KS |
|-------|--------|--------|--------|--------|--------|
| 111 | 158.55 | 155.80 | 156.17 | 157.68 | 156.22 |
| 200 | 14.86 | 11.22 | 11.44 | 11.72 | 11.15 |
| 220 | 189.80 | 189.79 | 189.05 | 191.14 | 189.48 |
| 311 | 129.10 | 125.90 | 125.03 | 126.40 | 125.50 |
| 222 | 11.63 | 10.33 | 9.82 | 9.61 | 9.50 |
| 400 | 162.31 | 162.13 | 161.39 | 163.57 | 162.51 |
| 331 | 109.55 | 109.47 | 109.39 | 111.13 | 110.34 |
| 420 | 12.09 | 11.59 | 11.29 | 10.85 | 11.08 |
| 422 | 140.56 | 143.30 | 142.82 | 145.37 | 144.43 |
| 440 | 128.76 | 128.86 | 128.29 | 131.05 | 130.19 |
| 531 | 88.37 | 88.29 | 87.81 | 89.74 | 89.18 |
| 620 | 117.46 | 117.28 | 116.57 | 119.37 | 116.78 |
| 533 | 80.77 | 80.73 | 80.26 | 82.25 | 80.46 |
| 622 | 12.28 | 12.26 | 12.17 | 12.15 | 12.11 |
| 444 | 107.69 | 107.78 | 107.04 | 109.80 | 107.37 |

^a See Ref. 26.

crystalline comparison. It is seen that for high k values the RHF results closely match experiment. According to Raccah,³³ this is usually the case. The KS and L results also closely match RHF and experiment at high k , while the S core is clearly several percent worse. At low k , where the valence wave functions are emphasized, the agreement with experiment is not impressive. All exchange approximations show an improvement over the free atomic RHF results because the SCOPW model allows the valence charge to spread out and redistribute. But even the best results, produced by the S approximation, are in poor agreement with experiment. The small deviation between the various approximations as compared to the discrepancy with experiment is again consistent with the weak dependence of binding energies on exchange. The SCOPW wave functions seem to depend much more weakly upon exchange constant than do the eigenvalues. But while S eigenvalues are clearly superior to the others, the wave functions are only slightly better, and the S binding energy band gap is slightly worse than the KS gap.

VI. CONCLUSIONS

The purpose of this paper was to examine the best known exchange approximations in both the atomic case and the crystalline case. We found that the atomic RHF results agreed very closely with experiment once corrections were made for core relaxation and the Lamb shift. An order-of-magnitude examination of the correction indicated that correlation corrections could be expected to be small relative to the energy deviations between the various exchange approximations in the atom. In the atomic case, the KS binding energies and the L results agreed well with the RHF results. Even these best exchange approximations gave total energies appreciably above the RHF total energy as measured by the S-KS difference in total energies.

In our SCOPW calculations, S eigenvalues gave the best results, while KS eigenvalues were too close

together and L eigenvalues were too spread out. However, the spread indicates that the L exchange is simulating the true HF results that one expects for the top valence band. To get results which match experiment, it appears that one must include an energy-dependent correlation term if HF exchange is used. Looking at the various binding energies calculated in the L approximation, one finds the energies again too spread out. The most interesting observation is that the S band energies match the measurements, and if one calculates exchange and correlation correctly, one may be led to a functional of the electron density similar to the S exchange. But in spite of the impressive agreement of the S eigenvalues with experiment, the S wave functions were not much better than the KS and the L wave functions.

It must be kept in mind when comparing crystalline results with experiment that defects in the calculational model can give rise to effects which can be compensated for by changing the exchange coefficient. An example is the widening of the bands caused by the use of a non-self-consistent superposition of atomic potentials. This widening relative to using a self-consistent potential can be corrected for by decreasing the exchange coefficient. Hidden deficiencies in our SCOPW model could cause similar misinterpretations. Consequently, we hope that other crystalline exchange studies will be undertaken using different models so that the results can be compared with ours. But based upon the results reported here, we are forced to conclude that a satisfactory completely first-principles energy-band model still does not exist. The joint problem of crystalline exchange and correlation requires deeper investigation.

ACKNOWLEDGMENTS

We would like to thank Dr. D. A. Liberman for making his relativistic atomic programs available to us. We are also grateful to Gene Johnson for his expert drafting of the figures. We would like to thank Dr. D. J. MacNaughton for his critical comments. One of us (VHS) would like to thank the National Research Council of Canada for an operating grant.

³³ P. M. Raccah (private communication).